On Sampling Strategies and Interpolation Schemes for Satellite-Tracked Drifters

STEVEN J. BOGRAD

Department of Earth and Ocean Sciences, University of British Columbia, Vancouver, British Columbia, Canada

ALEXANDER B. RABINOVICH AND RICHARD E. THOMSON

Institute of Ocean Sciences, Sidney, British Columbia, Canada

A. JANE EERT

Channel Consulting, Victoria, British Columbia, Canada

(Manuscript received 7 September 1997, in final form 16 July 1998)

ABSTRACT

The effects of reduced sampling schedules (duty cycles) on velocity statistics derived from satellite-tracked drifters in the northeast Pacific Ocean are investigated. Continuous segments of the drifter records (in which all available satellite positions fixes are recorded and processed by Service ARGOS) are degraded to match the standard duty cycle used in the World Ocean Circulation Experiment–Surface Velocity Program, in which there are 48 h of no data transmission followed by 24 h of received transmission (48–24 h). Also examined are duty cycles of 32–16 h and 16–8 h. It is found that the strong inertial motions prevalent in the drifter records result in significantly biased statistics derived from the degraded series. Reproduction of the original prime (mean and standard deviation) and rotary spectral statistics requires an interpolation that takes into account the oscillatory component of the drifter motions. Duty cycles having shorter but more frequent gaps (e.g., 16–8 h) are not sufficient to resolve the main features of the flow. The authors recommend that interpolations over duty cycle segments of drifter records be customized to account for the dominant modes of variability observed in available continuous segments.

1. Introduction

The World Ocean Circulation Experiment (WOCE)–Surface Velocity Program (SVP) provides observations of mixed layer velocity and sea surface temperature in all major ocean basins through deployments of satellite-tracked drifters. As part of the Canadian contribution to the SVP, more than 60 drifters were released north of 40°N in the North Pacific in 12 deployments between August 1990 and November 1994 (Bograd et al., 1999). An initial analysis of these data revealed strong inertial and semidiurnal motions, particularly for those drifters deployed in the Gulf of Alaska (Thomson et al. 1998). A question that arises is whether the standard sampling strategy employed in WOCE–SVP, in which there are 48 h of no data transmission obtained from the drifter followed by 24 h of received transmission (48–24 h), yields sufficiently accurate velocity statistics when high-frequency motions dominate.

Although drifters are relatively inexpensive compared to current meters, large numbers are needed to effectively sample basin-scale oceanic regions. More importantly, the cost of locating the drifters and transmitting the data (paid to Service ARGOS) can be prohibitively expensive. As pointed out by Hansen and Herman (1989), operating costs (i.e., daily data collection) far exceed the production costs of a drifter. An ideal arrangement would include a sufficient number of concurrently transmitting drifters maintained at a reduced sampling schedule, so as to derive statistically reliable circulation and temperature measurements at a minimum cost.

Using data from drifters drogued at 10–30-m depth in the tropical Pacific between 1979 and 1984, Hansen and Herman (1989) studied the effect of reducing the number and frequency of ARGOS transmissions on the retrieved current and temperature information. They found that transmission rates of one out of three days yielded acceptable velocity errors of ± 5 cm s^{-1} for equatorial regions just south of the equator. North of

Corresponding author address: Steven Bograd, Scripps Institution of Oceanography, Mail Code 0230, 9500 Gilman Drive, University of California, San Diego, La Jolla, CA 92093-0230.
E-mail: bograd@bowfell.ucsd.edu

the equator, due to enhanced mesoscale variability, this standard could not be met with a reduction to even one out of two days. The standard for sea surface temperature could be met throughout the sampled region with transmissions on one out of four days. This two-days-off/one-day-on transmission schedule (duty cycle) was adopted as the SVP standard.

While this sampling strategy has led to a significant reduction in operating costs and has enabled the deployment of a large number of drifters in each ocean basin, per SVP objectives, it is not necessarily the best duty cycle for all basins. Results are clearly dependent on the dynamics of the particular region sampled (e.g., Hansen and Herman 1989). In middle and high latitudes, inertial and tidal motions can dominate the flow variability (McNally et al. 1989; Thomson et al. 1997, 1998). Thus, it might be expected that the standard duty cycle, with its regular 48-h data gaps, will not provide sufficiently accurate current measurements when strong high-frequency motions prevail. Although these motions are not important for climate research, they are of intrinsic interest, and drifter ensembles *can* be used to investigate high-frequency current variability (Thomson et al. 1998).

In this study, we examine the effects of the standard duty cycle, as well as two other duty cycles (32–16 h and 16–8 h), on the velocity statistics derived from SVP drifters in the northeast Pacific. In particular, our goals are to (a) demonstrate what effects the duty cycle gaps have on velocity statistics derived from the drifter trajectories and (b) propose a relatively simple means of suppressing the negative effects of the duty cycle gaps. We proceed by degrading continuous segments (in which all available satellite position fixes are recorded and processed by Service ARGOS) of each drifter series to match those of the duty cycles and then we compare the prime (mean and standard deviation) and rotary spectral statistics derived from the series. We show that reproduction of the original prime and spectral statistics requires an interpolation that takes into account the oscillatory component of the drifter motions. The following section describes the dataset used in this study and the degradation and interpolation procedures applied to the original drifter series. This is followed by a comparison of the derived prime and spectral velocity statistics and a recommendation regarding sampling and interpolation strategies to be used in future drifter studies.

2. Data and methods

a. Drifter series

We demonstrate the effects of the duty cycles on the derived velocity statistics by focusing on the trajectories of six drifters deployed in the vicinity of station P (50°N, 145°W) in the northeast Pacific Ocean in September 1990 (Fig. 1a). Each drifter was equipped with a holey sock drogue centered 15 m below the surface. Strong high-frequency oscillations occur in the trajectories of each of these drifters. Inertial currents accounted for 58% of the total variance measured by these drifters, and semidiurnal currents accounted for another 11% (Thomson et al. 1998). For comparison, we also analyze the trajectory of a drifter, deployed near the head of the Gulf of Alaska in September 1992, which appeared to have weak inertial motions (Fig. 1b).

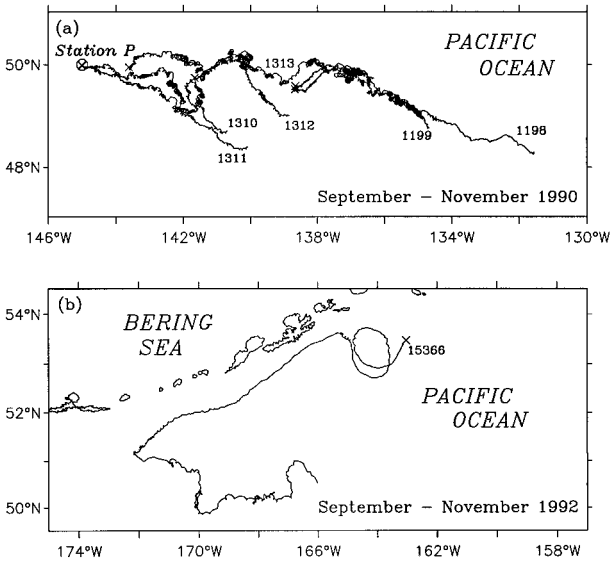

FIG. 1. Spaghetti diagram showing the first 90 days of the trajectories of (a) six drifters deployed near station P (50°N, 145°W) in the northeast Pacific in September 1990, which had strong inertial motions, and (b) a drifter deployed at the head of the Gulf of Alaska in September 1992, which had weak inertial motions.

The drifters studied here alternated between continuous data receive/transmit mode and the 48–24-h duty cycle at 90-day intervals. After the second 90-day period of continuous transmission, they remained on the 48–24-h duty cycle for the remainder of their lifetimes. Consequently, all reference statistics are derived using only the first 90-day period of each drifter's record.

b. Time series degradation

Each of the original drifter trajectories consisted of irregularly spaced time series of longitude and latitude. During the first 90-day period analyzed, the drifters in the station P group averaged 10.7 position fixes per day for an average of 964 data points per drifter record. Each time series was degraded to match the standard duty cycle, 48–24 h, as well as duty cycles of 32–16 and 16–8 h. The 48–24-h duty cycle reduced the average number of observations by 70%, while the 32–16- and 16–8-h duty cycles resulted in an average reduction of 72% and 76%, respectively. As illustrated by trajectory plots of the original and degraded series of drifters 1310 and 15366 (Figs. 2 and 3), some of the gaps in the duty cycle data are quite extensive. Especially large gaps are found in the 48–24-h degradation of drifter 15366 when it was within the fast-flowing Alaskan Stream (Fig. 3b).

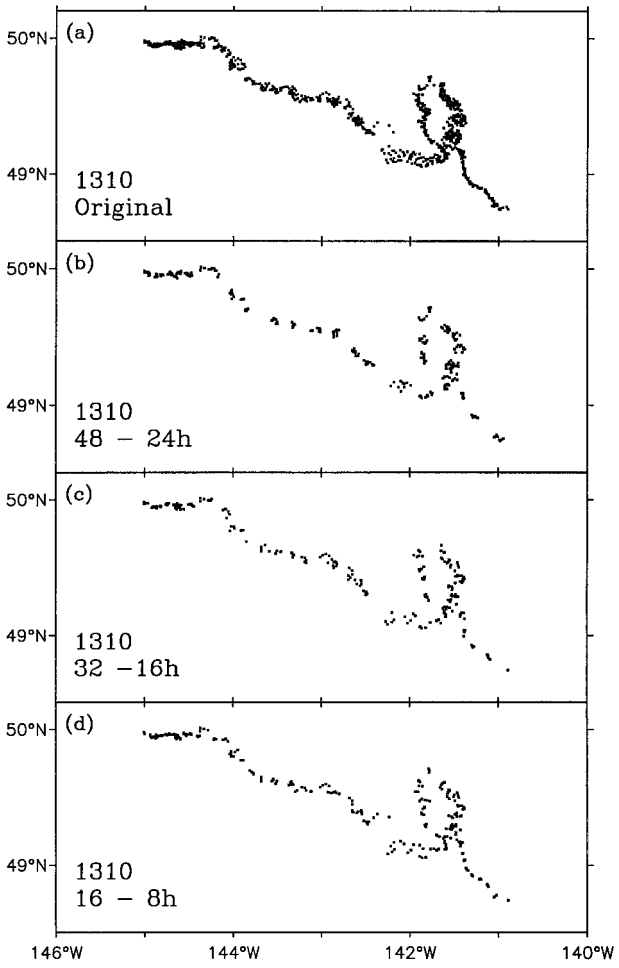

FIG. 2. The 90-day uninterpolated trajectories of drifter 1310 from (a) the original series, (b) 48–24-, (c) 32–16-, and (d) 16–8-h degraded series. Each mark represents an observation point. The number of observations contained in each series is (a) 947, (b) 287, (c) 239, and (d) 265.

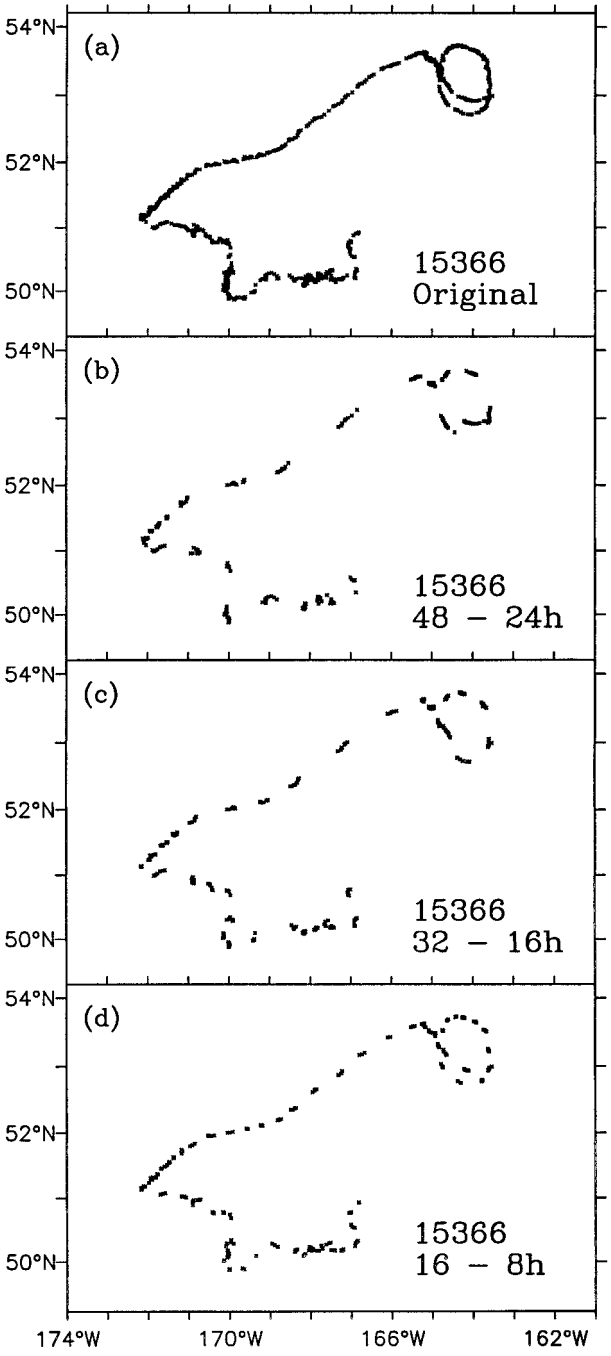

FIG. 3. As in Fig. 2, but for drifter 15366. The number of observations contained in each series is (a) 793, (b) 236, (c) 250, and (d) 235.

c. Time series interpolation

We used two distinct interpolation routines on the original and degraded series of each drifter in an attempt to reproduce the velocity statistics of the original series. We are interested in statistics in both the time domain (means and standard deviations, which we refer to as prime statistics) and the frequency domain (rotary spectra and frequency-partitioned rotary variances). The first fitting routine used was a Hermite spline, while the second assumed an oscillation of unknown frequency in the drifter motions and constructed a data-density-dependent local fit to the observations. The latter interpolation, referred to here as the multifunctional fit (MFF), is described below.

First, the average data density (number of observations per day) over a 3-day period was calculated starting at each observation point in the time series. The ''local'' interpolation of a selected segment of the series was then dependent on its data density. For a density of greater than 6 (fewer than 6) observations per day, the maximum number of observations allowed in the local interpolation was 30 (18). The maximum time and distance allowed in the segment was set at 10 days and 300 km, respectively. These criteria, based on trial and error with the datasets, were intended to ensure good

fits both for continuous and duty cycle segments. They represent a compromise between maintaining statistical stationarity within the segment (the desire to have a short segment) and having significantly more observation points than degrees of freedom (the desire to have a long segment). Data points were added to the local segment until any one of the limits (maximum number of observations, maximum distance or time) was met. The selected segment was then transferred to the fitting routine.

The function $\hat{p}(t)$, chosen to fit the selected segment, consisted of a polynomial plus an oscillation whose frequency, ω, was one of the parameters determined by the interpolation:

$$\hat{p}(t) = a + bt + ct^2 + dt^3 + et^4 + h \sin(\omega t + \phi), \quad (1)$$

where t is time, a–e are constants of the polynomial component, h is a constant, and ϕ is the phase lag for the oscillatory component. A gradient-expansion algorithm was applied (Bevington 1969). This algorithm expands the fitting function $\hat{p}(t)$ as a function of the parameters ($a, b, \ldots, \omega, \phi$) and uses the method of least squares to determine the optimum value for the parameter increments in a gradient search. The resulting fit to the local data segment was then subsampled at 3-hourly intervals. In a broad sense, the polynomial fits the general trend of the segment, while the oscillation fits the dominant high-frequency fluctuations.

The order of the polynomial depends on the data density of the segment. If the selection process resulted in only a few observations in the segment (e.g., if the maximum distance or time limit was met during a duty cycle portion of the series), a fourth-order polynomial might result in an unstable fit (a curve oscillating wildly between the data points). If this was the case, a smaller-order polynomial was used instead. For the trajectories fitted here, a quartic polynomial was generally required. A new segment was then selected by advancing the start time by eight points for a high-density segment (>six observations per day) or by two points for a low-density segment (<six observations per day), and repeating the selection and fitting procedure described above. The overlapping segments yielded multiple predicted fits at each 3-hourly time.

Once the entire series had been covered, two different approaches were used to obtain the final interpolated series. In the first method (MFF1), all overlapping fitted segments at each 3-hourly time were averaged to get a single estimate of drifter position (latitude, longitude). Velocity components were then calculated by first differencing the position data. In the second method (MFF2), instead of averaging overlapping segments, the predicted location at a given time that had the lowest root-mean-square distance to the neighboring three observation points on either side of that time (i.e., the ''best'' fit, in a least squares sense) was chosen. Velocity components were again calculated by first differencing the position data.

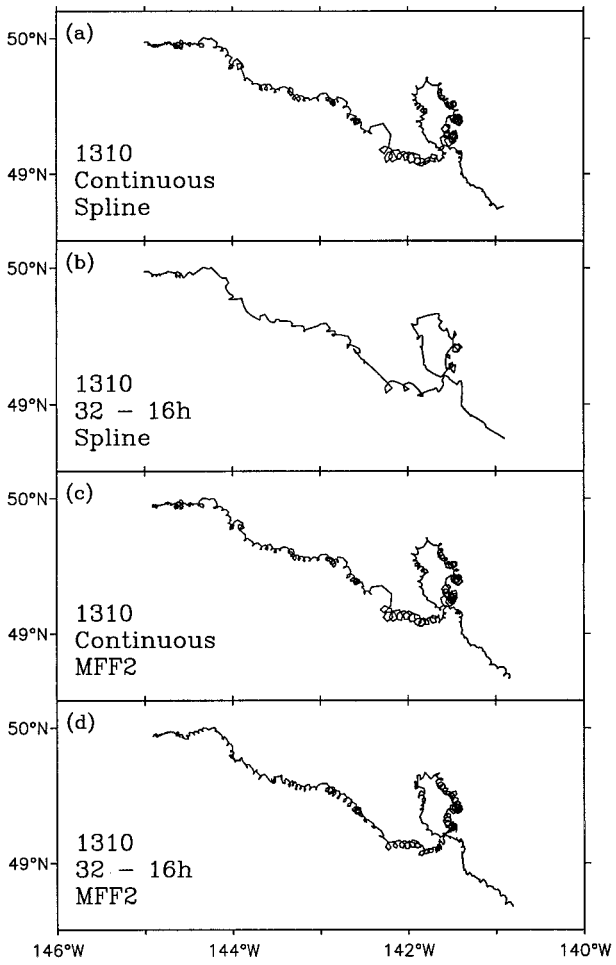

FIG. 4. The 90-day interpolated trajectories of drifter 1310 from (a) the spline-interpolated original series, (b) the spline-interpolated 32–16-h degraded series, (c) the MFF2-interpolated original series, and (d) the MFF2-interpolated 32–16-h degraded series.

The respective spline and MFF2 interpolations applied to the continuous and 32–16-h degraded series of drifters 1310 and 15366 are shown in Figs. 4 and 5. The similarity of the spline and MFF2 (and MFF1, not shown) interpolations of the continuous series (i.e., the original undegraded series; e.g., Figs. 4a,c) demonstrate the effectiveness of each of the fitting routines for trajectories unaffected by duty cycle gaps. This gives us confidence in our ability to compare the interpolation schemes using the degraded series. The spline interpolation of the 32–16-h degraded series does not reproduce the high-frequency motions seen in the original series (Fig. 4b), while oscillations of inertial period *were* reproduced in the MFF2-interpolated degraded series of drifter 1310 in regions where strong inertial motions were originally observed (Fig. 4d).

Positions were also estimated and velocity components calculated at 6-hourly intervals (not shown),

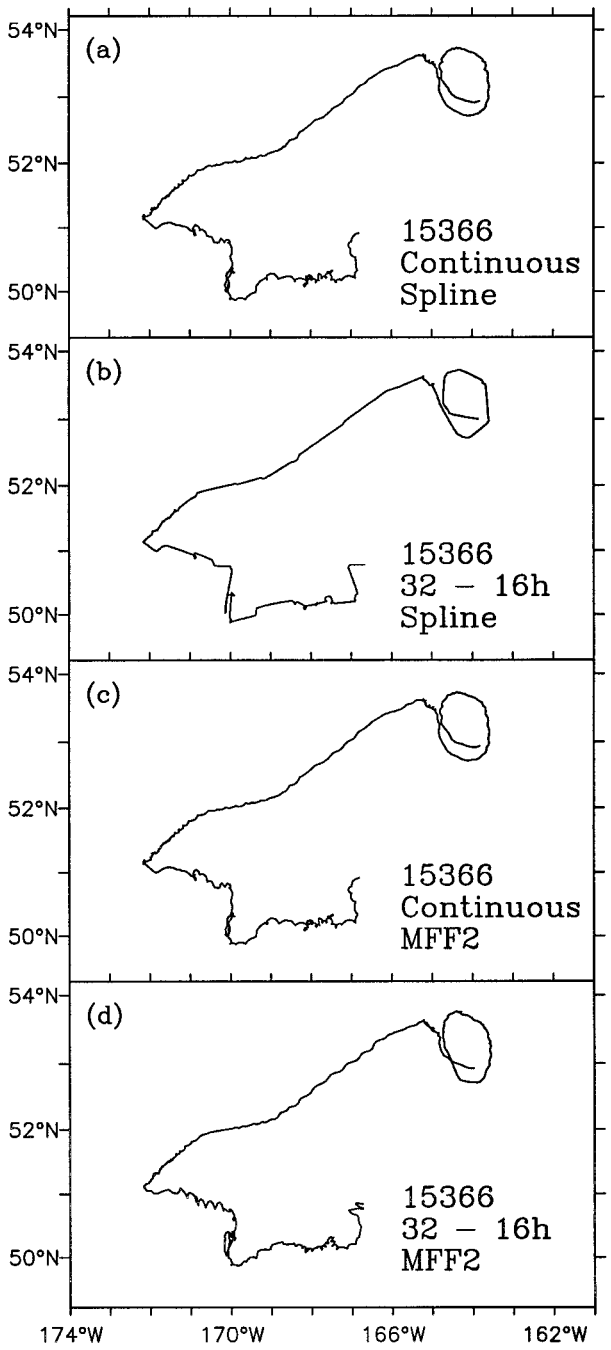

FIG. 5. As in Fig. 4, but for drifter 15366.

which is consistent with the standard product available from the SVP Data Assembly Center. However, because 10 or more observations per day are typically available from continuous drifter segments at extratropical latitudes, it was more appropriate to subsample the interpolation at 3-hourly intervals. Furthermore, 6-hourly data contain 2.5 data points or less per inertial period at middle to high latitudes and have a Nyquist period of 12 h, that is, semidiurnal. Given the significant energy levels at the inertial and semidiurnal periods that are commonly observed in the upper ocean, the higher sampling rate seems particularly desirable.

3. Results

a. Prime statistics

Prime velocity statistics provide a direct comparison between the original and degraded series. As Table 1 indicates, the degradations, when left uninterpolated, give somewhat different mean velocities from the original series. This is most likely due to overestimated first-differenced speeds for position fixes closely spaced in time. However, the original mean speeds were quite adequately reproduced for each of the degradations after they were interpolated with the spline, MFF1, or MFF2 algorithms (Table 1). All of the degradations of drifter 1310 have mean velocity components within 1% of the original for each of the interpolations. Similar comparisons can be made for each of the station P drifters (not shown).

The standard deviations (variances) of the current velocities derived from the spline-interpolated degraded series of drifter 1310 were approximately 50% (70%) smaller than those derived from the spline-interpolated original series, while those calculated from the MFF1 interpolation were 30% (50%) smaller (Table 1a). Similar results were found for drifter 15366, although the differences between the original and degraded variances were smaller (Table 1b). The MFF2 interpolation, however, yielded standard deviations (variances) within 5% (10%) of the original for both drifters 1310 and 15366. Only the meridional variance of the 16–8-h degradation of drifter 15366 was strongly overestimated. Thus, although each of the interpolations of the degraded series reproduced the mean velocity components of the original series, only the MFF2 interpolation yielded variances comparable to those of the original. This was most dramatically demonstrated by the drifters containing strong inertial oscillations.

In many applications (e.g., in the SVP) it is the long-term circulation statistics derived from an ensemble of drifters (not necessarily operating simultaneously) that are desired. A question is whether the gaps from the duty cycle, and their subsequent interpolation, can affect these ensemble statistics. For each of the uninterpolated and interpolated series in the station P group, the ensemble velocity statistics were derived using the daily averaged series from all six drifters (i.e., all data points, if any, from each Julian day were averaged before calculating a 90-day ensemble mean). The results (not shown) are similar to those derived from the individual drifters. The degradations did introduce small errors in the ensemble mean velocities and standard deviations, but each of the interpolation schemes was able to adequately reproduce the statistics (means *and* variances) derived from the original ensemble. We note that increased time averaging will yield low variances and that

TABLE 1. Means (overbar) and standard deviations of the east–west (u) and north–south (v) currents, including the 95% confidence intervals, derived from the uninterpolated, spline-interpolated, and MFF-interpolated series of (a) a drifter with strong inertial motions (1310) and (b) a drifter with weak inertial motions (15366). Mean velocity components are the 90-day averages derived from the first-differenced components calculated at each observation point.

	Uninterpolated	Spline	MFF1	MFF2
(a) Drifter 1310				
$\overline{u}$ (cm s^{-1})				
Original	3.93 ± 1.47	3.89 ± 1.37	3.91 ± 1.44	3.90 ± 1.35
48–24 h	4.04 ± 2.25	3.87 ± 0.69	3.85 ± 1.02	3.89 ± 1.41
32–16 h	4.20 ± 2.58	3.91 ± 0.68	3.90 ± 0.96	3.94 ± 1.23
16–8 h	4.38 ± 2.72	3.90 ± 0.75	3.89 ± 1.09	3.92 ± 1.24
$\overline{v}$ (cm s^{-1})				
Original	−2.14 ± 1.39	−1.80 ± 1.40	−1.84 ± 1.47	−1.90 ± 1.38
48–24 h	−1.21 ± 2.26	−1.81 ± 0.70	−1.81 ± 0.94	−1.89 ± 1.37
32–16 h	−2.41 ± 2.71	−1.82 ± 0.73	−1.81 ± 1.08	−1.89 ± 1.32
16–8 h	−2.66 ± 2.46	−1.82 ± 0.69	−1.82 ± 1.20	−1.88 ± 1.33
$\sqrt{\overline{u'^2}}$ (cm s^{-1})				
Original	23.07 ± 1.04	18.57 ± 0.97	19.43 ± 1.02	18.19 ± 1.35
48–24 h	19.00 ± 1.56	9.38 ± 0.49	13.75 ± 0.72	18.91 ± 0.99
32–16 h	19.77 ± 1.79	9.22 ± 0.48	13.01 ± 0.68	16.49 ± 0.87
16–8 h	21.67 ± 1.89	10.15 ± 0.53	14.80 ± 0.77	16.64 ± 0.88
$\sqrt{\overline{v'^2}}$ (cm s^{-1})				
Original	21.88 ± 0.99	18.92 ± 0.99	19.92 ± 1.04	18.56 ± 1.38
48–24 h	19.01 ± 1.56	9.49 ± 0.50	12.70 ± 0.67	18.45 ± 0.97
32–16 h	20.76 ± 1.88	9.83 ± 0.51	14.61 ± 0.76	17.74 ± 0.93
16–8 h	19.55 ± 1.70	9.36 ± 0.49	16.17 ± 0.85	17.91 ± 0.94
(b) Drifter 15366				
$\overline{u}$ (cm s^{-1})				
Original	−2.94 ± 2.15	−3.27 ± 2.26	−3.33 ± 2.22	−2.30 ± 2.27
48–24 h	−3.23 ± 4.29	−3.05 ± 1.89	−2.61 ± 2.03	−2.50 ± 2.19
32–16 h	−2.89 ± 3.86	−3.10 ± 1.95	−3.33 ± 1.94	−2.44 ± 2.39
16–8 h	−2.78 ± 4.32	−3.27 ± 1.95	−3.27 ± 2.00	−2.35 ± 2.43
$\overline{v}$ (cm s^{-1})				
Original	−3.78 ± 1.97	−3.65 ± 2.12	−3.51 ± 2.10	−3.83 ± 2.13
48–24 h	−3.99 ± 3.70	−3.66 ± 1.63	−3.46 ± 1.87	−3.57 ± 2.31
32–16 h	−3.54 ± 3.66	−3.89 ± 1.65	−3.72 ± 1.68	−3.66 ± 2.30
16–8 h	−3.83 ± 3.59	−3.64 ± 1.69	−3.56 ± 1.82	−3.61 ± 2.89
$\sqrt{\overline{u'^2}}$ (cm s^{-1})				
Original	30.83 ± 1.52	28.22 ± 1.60	27.55 ± 1.57	28.45 ± 1.60
48–24 h	32.31 ± 2.98	23.61 ± 1.34	25.28 ± 1.44	27.38 ± 1.55
32–16 h	29.56 ± 2.68	24.41 ± 1.38	24.26 ± 1.37	29.97 ± 1.69
16–8 h	31.52 ± 2.99	24.37 ± 1.38	24.96 ± 1.41	30.47 ± 1.72
$\sqrt{\overline{v'^2}}$ (cm s^{-1})				
Original	28.23 ± 1.39	26.50 ± 1.50	26.17 ± 1.49	26.73 ± 1.51
48–24 h	27.82 ± 2.56	20.35 ± 1.15	23.31 ± 1.33	28.84 ± 1.63
32–16 h	25.80 ± 2.34	20.66 ± 1.17	21.02 ± 1.19	28.81 ± 1.63
16–8 h	26.22 ± 2.49	21.16 ± 1.20	22.78 ± 1.29	36.30 ± 2.05

any of the interpolation schemes applied to the duty cycle segments will produce similar statistics. Hence, for climate studies, the duty cycle gaps should not be problematic.

b. Rotary spectral analysis

A decomposition of Cartesian velocity components $[u(t), v(t)]$ into polarized rotary components $[u^-(t), u^+(t)]$ is an ideal method for analyzing motions in which one component is expected to be dominant (e.g., Gonella 1972; Mooers 1973). Here, $u^-(t)$ and $u^+(t)$ are the clockwise and counterclockwise components, respectively. Spectral estimates, $S(\omega; u^{\pm})$, were obtained for each drifter, with each data segment weighted using a Kaiser–Bessel window (Harris 1978) prior to the Fourier transform and half-window overlapping performed to increase the number of degrees of freedom. The rotary variances of the components,

$$\mathrm{var}(u^-, u^+) = \int_{\Delta\omega} [S(\omega; u^-), S(\omega; u^+)]\, d\omega, \quad (2)$$

$$\mathrm{var}_{\mathrm{tot}} = \mathrm{var}(u^-) + \mathrm{var}(u^+), \quad (3)$$

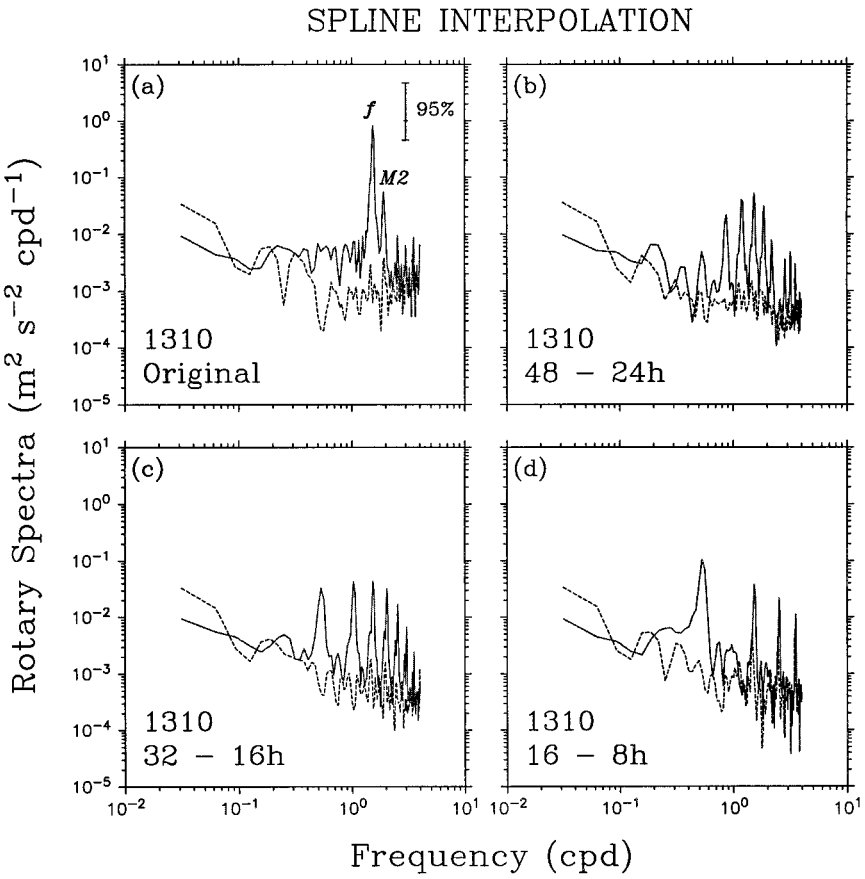

FIG. 6. The clockwise (S^-; solid line) and counterclockwise (S^+; dashed line) rotary energy density spectra ($m^2\ s^{-2}\ cpd^{-1}$) derived from the first 80-day period of the spline-interpolated series of drifter 1310 for (a) the original series, (b) the 48–24-, (c) the 32–16-, and (d) the 16–8-h degraded series. The 95% confidence limits and the inertial (f) and semidiurnal (M2) peaks are shown in (a).

were then estimated, where the bandwidth $\Delta\omega$ encompasses a specified range of frequencies.

Rotary energy density spectra of the spline-interpolated original and degraded series of drifter 1310 are provided in Fig. 6. For the original series, the motions are nearly isotropic at the lowest frequencies (periods $>$ 4 days) and are anticyclonically polarized at periods of 12 h to 4 days (Fig. 6a). There is a significant clockwise peak at the inertial frequency (period approximately 15.7 h at this latitude) and a weaker semidiurnal (M2) peak (12.4 h). The spectra are noisy at high frequencies.

The spectra derived from the spline-interpolated degraded series reveal a very different picture (Figs. 6b,c,d). The clockwise spectra have numerous spurious peaks that are as strong as, or stronger than, the inertial peak. These peaks correspond to inertial energy that has been aliased to multiples of the duty cycle frequency $f_i \pm nf_{dc}$, where f_i is the inertial frequency (approximately 1.53 cpd), f_{dc} is the duty cycle frequency [e.g., $1/(32h + 16h) = 0.5$ cpd for the 32–16-h degradation], and $n = 1, 2$, etc. Some energy from the weaker M2 peak has likely been aliased to lower frequencies as well. The aliasing is especially problematic in the spectra of the 16–8-h series (Fig. 6d), where a strong clockwise peak centered at two days contains a significant portion of the total energy. Thus, the mesoscale energy distribution (2–5 days) is significantly affected by this duty cycle.

D'Asaro (1992) found spectral leakage due to the inherently clustered nature of the ARGOS position fixes for drifters deployed during the OCEAN STORMS experiment. This is related to the orbital characteristics of the satellite. The aliasing observed here is due solely to the interaction of strong inertial motions with the duty cycle, which is a potentially tractable problem. Specifically, the user cannot control *when* the satellite position fixes are available, but can, to some degree, control the duty cycle that optimizes the data records.

The MFF interpolations solve the problem of aliasing by the duty cycle. The MFF1 interpolation (not shown) adequately reproduces the inertial peak in the degraded series, but fails in that the clockwise energy at periods less than inertial and from 1–5 days is two orders of magnitude lower than for the original series. This is the ''missing energy'' seen in the standard deviations of the degraded series (Table 1a).

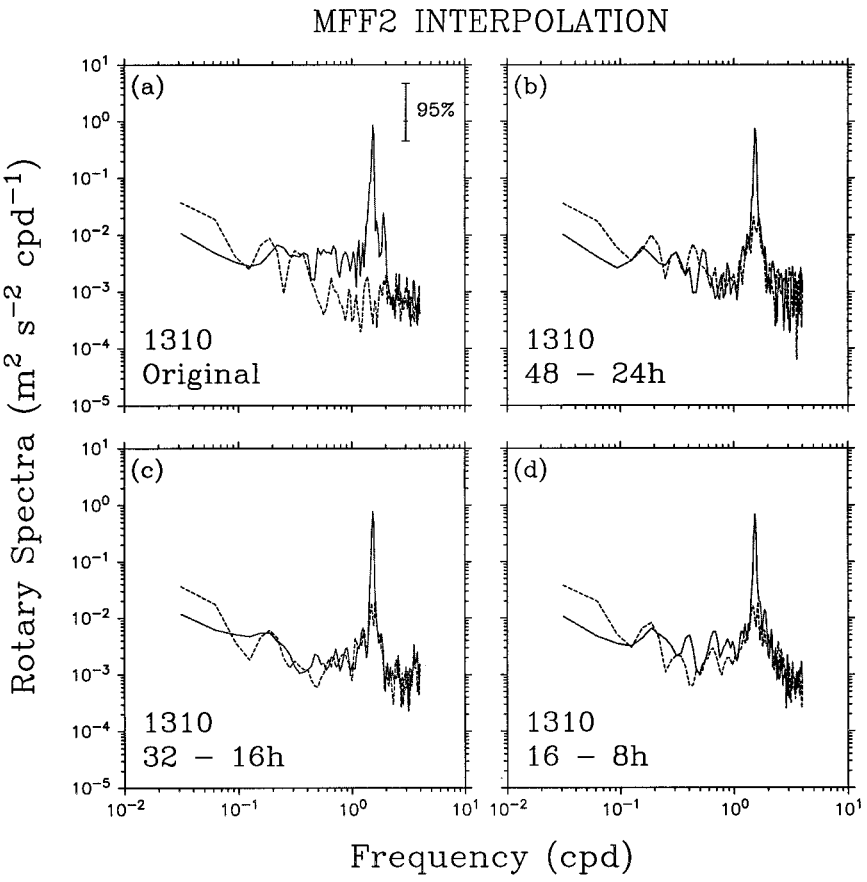

FIG. 7. As in Fig. 6 but for the MFF2-interpolated original and degraded series of drifter 1310.

The rotary spectra of the MFF2-interpolated original and degraded series of drifter 1310 (Fig. 7) demonstrate the effectiveness of the MFF2 interpolation. The spectra of each of the degraded series (Figs. 7b,c,d) match the spectra of the original series (Fig. 7a) reasonably well. The primary differences between the original and degraded MFF2 spectra are the stronger S^+ inertial peaks in the latter (but still two orders of magnitude smaller than the S^- peak), which are due to fitting the zonal (longitude) and meridional (latitude) components independently using (1), thereby losing the phase information of the inertial motions. The spectra of the 48–24- and 16–8-h degradations are noisy at periods less than 12 h, while those of the 32–16-h degradation appear to most closely resemble the spectra of the original series, with an energy roll-off at high frequencies.

The rotary spectra of the MFF2-interpolated original series of drifter 15366 (Fig. 8a) have a broad clockwise peak centered between the inertial and M2 frequencies and are weakly anticyclonically polarized at low frequencies, with S^+ troughs at periods of 2.5 and 5.5 days. The low frequencies are significantly more energetic here than in the station P group. The spectra of the 32–16-h degradation (Fig. 8c) appear to most closely resemble the spectral characteristics of the original series, although the S^- near-inertial peak is overestimated and too narrow. This is due to fitting only one oscillation in the interpolation. Adding a prescribed M2 oscillation and fitting the (varying) inertial oscillation would likely improve the spectral characteristics. The spectra of the 48–24-h degradation are very noisy at high frequencies (Fig. 8b), while *only* the low frequencies (periods > 1 day) of the original spectra are reproduced in the 16–8-h degradation (Fig. 8d). The spectra of the spline interpolations of drifter 15366 (not shown) are adequate for the original series, but again yield significant spectral leakage in the degraded series.

4. Discussion

A question raised by this analysis is whether one of the three investigated duty cycles is better suited for midlatitude drifters in regions of strong inertial oscillations. A comparison of the rotary variances computed in four frequency bands for the MFF2-interpolated original and degraded series of the station P ensemble allows for a more quantitative comparison of the spectral statistics (Table 2). The energy contained in the mesoscale

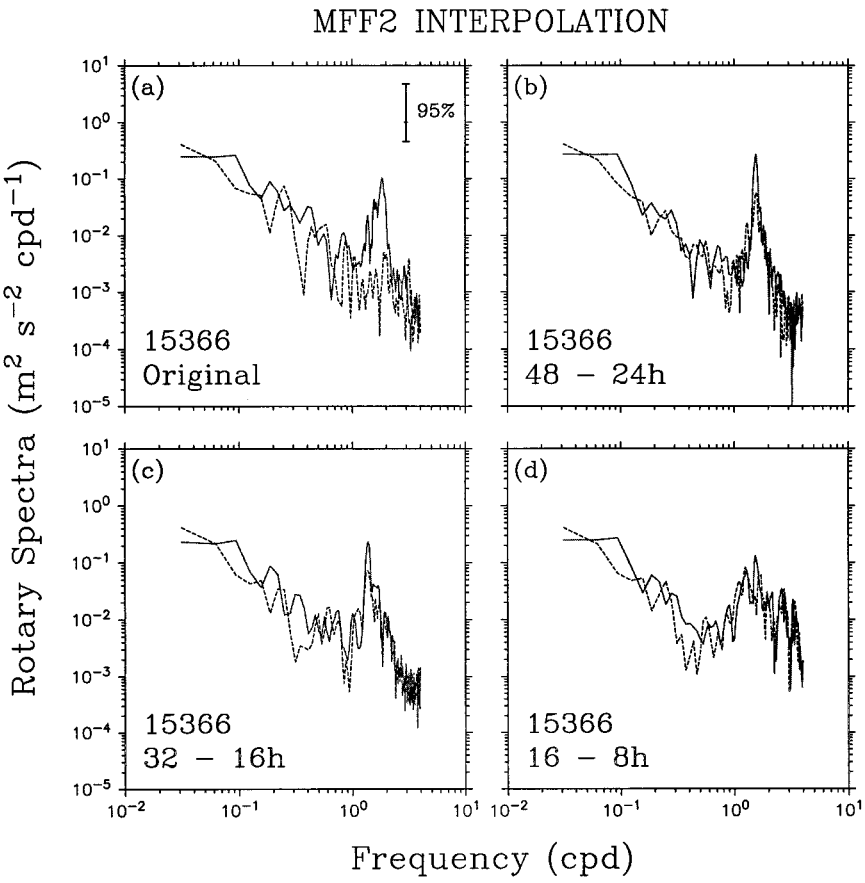

FIG. 8. As in Fig. 6 but for the MFF2-interpolated original and degraded series of drifter 15366.

band (2–8-day period), and its partition between the clockwise and counterclockwise components, is similar for the original and each of the degraded series. The 48–24-h degradation has too much counterclockwise energy at the highest frequencies, while the 16–8-h degradation has too much high-frequency energy in both rotary components. The overestimated high frequency energies are also seen in the MFF2-interpolated spectra of drifter 1310 (Figs. 7b,d). The 16–8-h degradation also has too much counterclockwise energy in the subinertial band (17-h–1.9-day period). In general, it appears that the 32–16-h degradation reproduces the total energy of the original series, and its frequency partition, very well. Although the MFF2 routine slightly overestimates the counterclockwise energies at the expense of the clockwise energies in the subinertial and high-frequency bands, these bands contain a relatively small portion of the total energy (10%–15%). Fitting the position data as a complex series could improve the frequency partitioning of the rotary variances.

Further comparison of the duty cycles can be made by computing the rotary coefficient, given by

$$r(\omega) = \frac{S(\omega; u^-) - S(\omega; u^+)}{S(\omega; u^-) + S(\omega; u^+)}, \qquad (4)$$

for the station P ensemble (Table 3). For clockwise (counterclockwise) rotary motions, r is positive (negative), and $(-1 \leq r \leq 1)$ (Thomson et al. 1998). For each of the duty cycles, the rotary coefficient is too low in all frequency bands, indicating an excess (deficiency) of counterclockwise (clockwise) energy in the interpolations of the degraded series. Thus, effects of the duty cycle are prevalent even at relatively low frequencies, where clockwise energies are underestimated in the mesoscale band and counterclockwise energies are overestimated in the subinertial band (see Table 2). The rotary coefficients derived from the 32–16-h degradations are in closest agreement with those of the original series, particularly in the near-inertial frequency band, which contained nearly 80% of the total energy of the motions with periods less than 8 days.

Since clockwise oscillatory motions dominate the station P ensemble, we can also look at the clockwise spectral amplitude ratios between the original and degraded series in each of the four frequency bands and for all three interpolation algorithms (Table 4). The spline interpolation clearly does not reproduce the inertial motions. The MFF1 interpolation yields the inertial peak but does not have nearly enough clockwise

TABLE 2. Clockwise [$S^-(\omega)$], counterclockwise [$S^+(\omega)$], and total [$S_{tot}(\omega)$] rotary variance in four frequency bands derived from the MFF2-interpolated series of the station P ensemble. Numbers in parentheses refer to the percentage of the total rotary variance. The frequency bands are mesoscale (periods of 2–8 days), subinertial (periods of 17 h–1.9 days), near inertial (periods of 14.7–16.8 h), and high (periods of 6–14.5 h).

	Original	48–24 h	32–16 h	16–8 h
$S^-(\omega)$ (cm^2 s^{-2}) (%)				
Mesoscale	23.1 (2.4)	13.4 (1.5)	14.4 (1.6)	13.1 (1.2)
Subinertial	63.9 (6.6)	34.6 (4.0)	43.3 (4.7)	56.4 (5.0)
Near-inertial	765.5 (79.0)	625.0 (71.8)	705.1 (75.9)	673.4 (59.5)
High	64.7 (6.7)	60.8 (7.0)	47.7 (5.1)	125.0 (11.0)
$S^+(\omega)$ (cm^2 s^{-2}) (%)				
Mesoscale	11.1 (1.1)	13.1 (1.5)	10.4 (1.1)	10.0 (0.9)
Subinertial	7.8 (0.8)	27.7 (3.2)	27.5 (3.0)	48.3 (4.3)
Near-inertial	2.0 (0.2)	30.8 (3.5)	29.8 (3.2)	77.3 (6.8)
High	15.8 (1.6)	48.8 (5.6)	34.9 (3.8)	112.5 (9.9)
$S_{tot}(\omega)$ (cm^2 s^{-2}) (%)				
Mesoscale	34.2 (3.5)	26.5 (3.0)	24.8 (2.7)	23.1 (2.1)
Subinertial	71.7 (7.4)	62.3 (7.2)	70.8 (7.7)	104.7 (9.3)
Near-inertial	767.5 (79.2)	655.8 (75.3)	734.9 (79.1)	750.7 (66.3)
High	80.5 (8.3)	109.6 (12.6)	82.6 (8.9)	237.5 (20.9)

energy in the subinertial and high-frequency bands. The MFF2 interpolation adequately reproduces the clockwise rotary energy distribution in all frequency bands, with the 32–16-h degradation yielding the best comparison.

The MFF2 interpolation does not resolve the inertial and semidiurnal peaks in the degraded series (e.g., Fig. 7). Since inertial motions were nearly two orders of magnitude stronger than semidiurnal motions in the station P drifter records, we did not deem it necessary to attempt this resolution. Our main purpose was simply to suppress the effects of the duty cycle and reproduce the *dominant* motions in the degraded segments. The MFF interpolation can readily be made more sophisticated, depending on the nature of the data set and the user's interests. For example, one could add oscillations of known frequency if particular tidal components are known to dominate the motions, as was done by Pease et al. (1995). However, our results demonstrate that a relatively simple procedure can (and should) be applied to general drifter datasets, where high-frequency motions may or may not be strong (or may or may not be *known* to be strong), and the prime and spectral statistics can be confidently estimated for both continuous and duty cycle segments. We recommend that users ''learn'' from the continuous segments of their drifter trajectories (i.e., those not spoiled by the duty cycle) and subsequently customize their interpolation routine in order to adequately account for the dominant modes of variability over the duty cycle segments. Since all SVP drifters were drogued at a depth of 15 m, we expect the dominant mode of variability to be inertial oscillations.

Finally, we note that there could be limitations to our proposed method of suppressing the negative effects of the duty cycle gaps. If no continuous portion of a drifter

TABLE 3. The rotary coefficient in four frequency bands of the MFF2-interpolated series of the station P drifter ensemble. The frequency bands are the same as in Table 2.

	Original	48–24 h	32–16 h	16–8 h
$r(\omega)$				
Mesoscale	0.351	0.011	0.161	0.134
Subinertial	0.782	0.111	0.223	0.077
Near-inertial	0.995	0.906	0.919	0.794
High	0.607	0.109	0.155	0.053

TABLE 4. The clockwise (S^-) spectral amplitude ratios in four frequency bands, and for total clockwise energy, of the original to the degraded series for the spline-interpolated and MFF-interpolated series of the station P drifter ensemble. The frequency bands are the same as in Table 2.

	Original		
	48–24 h	32–16 h	16–8 h
Spline			
Mesoscale	1.7	1.2	0.7
Subinertial	0.8	0.9	1.0
Near-inertial	12.8	16.4	29.8
High	1.7	2.0	4.2
Total	3.8	4.4	5.8
MFF1			
Mesoscale	4.6	4.4	5.5
Subinertial	18.2	14.8	11.1
Near-inertial	1.2	1.4	1.3
High	24.7	32.2	5.6
Total	1.6	1.8	1.7
MFF2			
Mesoscale	1.7	1.6	1.8
Subinertial	1.8	1.5	1.1
Near-inertial	1.2	1.1	1.1
High	1.1	1.4	0.5
Total	1.2	1.1	1.1

record exists, or if the dynamics sampled by a drifter during a duty cycle portion are different from the dynamics prevalent during the initial continuous period (either due to changing seasons or because the drifter has entered a region with different mesoscale dynamics), it could be difficult to know how well the interpolation is reproducing the ''true'' trajectory. This is a problem inherent to time series with many gaps and emphasizes the potential impact the duty cycle can have when one is interested in investigating high-frequency currents.

5. Conclusions

Chereskin et al. (1989) explored the effects of upper-ocean vertical shear on drifter slippage, while D'Asaro (1992) analyzed the effects of inherent Service ARGOS sampling errors on drifter velocity estimates. In this study, we have examined the effects of reduced sampling schedules (duty cycles) on velocity statistics derived from satellite-tracked drifters in the northeast Pacific Ocean. Our findings show that both spline interpolation and more sophisticated multifunctional (MFF) interpolation of degraded (duty cycle) segments of continuous drifter trajectory records adequately reproduce the mean velocities of the original data series. This applies to the standard duty cycle used in most large-scale drifter deployments consisting of 48 h of no ARGOS data transmission followed by 24 h of ARGOS transmission received (48–24 h), as well as to duty cycles having shorter but more frequent gaps (32–16 and 16–8 h). However, our ability to reproduce the rotary spectral characteristics of the original time series, as well as the velocity variances, is strongly dependent on the interpolation scheme applied to the duty cycle record. The spline interpolation underestimated the velocity variances and produced numerous spurious spectral peaks, with inertial energy aliased to multiples of the duty cycle frequency. On the other hand, the MFF routine described here, which allows for an oscillatory component to the drifter motions, was able to adequately reproduce the velocity variances and rotary spectral features of the original data series for each of the three types of degraded series examined. Best reproduction of the rotary spectral amplitudes and associated frequency partitioning required that we select the best-fitted segments in the interpolation routine (MFF2) rather than average overlapping segments (MFF1). Nevertheless, even at subinertial frequencies, the duty cycle results in biased estimates of the rotary velocity variances. We expect that a more sophisticated fitting routine, which would allow for oscillations of known frequency in regions where specific frequency components (such as semidiurnal tidal motions) are known to dominate (cf. Pease et al. 1995), would further improve estimates of the spectral characteristics.

Results of our analysis also indicate that, for the three duty cycles investigated and for mid- to high- latitude drifter motions having strong inertial and/or semidiurnal motions, the spectral characteristics of the original continuous records are most consistently reproduced by the 32–16-h duty cycle. This presumably is because the 16-h transmission-received segments of drifter tracks are sufficiently long to define superinertial motions, while the 32-h transmission-blackout segments are short enough that the main features of the motions remain relatively unchanged. The duty cycle with the shortest and most frequent gaps (16–8 h) yielded the worst reproduction, with significantly overestimated superinertial energies.

Drifter engineering has progressed rapidly in recent years. Modern drifters are capable of measuring velocities and sea surface temperature to accuracies of 5 cm s^{-1} and 0.1° (Hansen and Poulain 1996), respectively, over a period greater than a year, and, in some circumstances, of obtaining useful information across entire basins well over a year after deployment (Thomson et al. 1997; Bograd et al., 1999). Consequently, drifter deployments have become an integral component of many large-scale and mesoscale observational studies. Drifters have also been effectively used to investigate high-frequency currents (Thomson et al. 1998). The user has the main obligation to generate reliable statistical information from the drifter data. In this regard, we strongly encourage users to take into account high-frequency motions during time series interpolation. In light of the results presented here, we further recommend that Service ARGOS 1) lower the costs of drifter tracking and data transmission, and 2) provide a selection of duty cycle options that depend on the latitude of the drifter deployments (specifically, equatorial versus nonequatorial deployments).

Acknowledgments. This work was supported by NSERC Grant CSP0100386 to Paul LeBlond (UBC) and NSERC Grant OGP0105562 to Richard Thomson. The comments of two anonymous reviewers helped improve the clarity of the presentation.

REFERENCES

Bevington, P. R., 1969: *Data Reduction and Error Analysis for the Physical Sciences.* McGraw-Hill, 336 pp.

Bograd, S. J., R. E. Thomson, A. B. Rabinovich, and P. H. LeBlond, 1999: Near-surface circulation of the northeast Pacific Ocean derived from WOCE–SVP satellite-tracked drifters. *Deep-Sea Res.,* in press.

Chereskin, T. K., P. P. Niiler, and P.-M. Poulain, 1989: A numerical study of the effect of upper-ocean shear on flexible drogued drifters. *J. Atmos. Oceanic Technol.,* **6,** 243–253.

D'Asaro, E. A., 1992: Estimation of velocity from Argos-tracked surface drifters during OCEAN STORMS. *J. Atmos. Oceanic Technol.,* **9,** 680–686.

Gonella, J., 1972: A rotary-component method for analyzing meteorological and oceanographic vector time series. *Deep-Sea Res.,* **19,** 833–846.

Hansen, D. V., and A. Herman, 1989: Temporal sampling requirements for surface drifting buoys in the tropical Pacific. *J. Atmos. Oceanic Technol.,* **6,** 599–607.

——, and P.-M. Poulain, 1996: Quality control and interpolations of

WOCE–TOGA drifter data. *J. Atmos. Oceanic Technol.,* **13,** 900–909.

Harris, F. J., 1978: On the use of windows for harmonic analysis with the discrete Fourier transform. *Proc. IEEE,* **66,** 51–83.

McNally, G. J., D. S. Luther, and W. B. White, 1989: The subinertial frequency response of wind-driven currents in the mixed layer measured by drifting buoys in the midlatitude North Pacific. *J. Phys. Oceanogr.,* **19,** 290–300.

Mooers, C. N. K., 1973: A technique for the cross spectrum analysis of pairs of complex-valued time series, with emphasis on properties of polarized components and rotary invariants. *Deep-Sea Res.,* **20,** 1129–1141.

Pease, C. H., P. Turet, and R. S. Pritchard, 1995: Barents Sea tidal and inertial motions from Argos ice buoys during the Coordinated Eastern Arctic Experiment. *J. Geophys. Res.,* **100,** 24 705–24 718.

Thomson, R. E., P. H. LeBlond, and A. B. Rabinovich, 1997: Oceanic odyssey of a satellite-tracked drifter: North Pacific variability delineated by a single drifter trajectory. *J. Oceanogr.,* **53,** 81–87.

——, ——, and ——, 1998: Satellite-tracked drifter measurements of inertial and semidiurnal currents in the northeast Pacific. *J. Geophys. Res.,* **103,** 1039–1052.